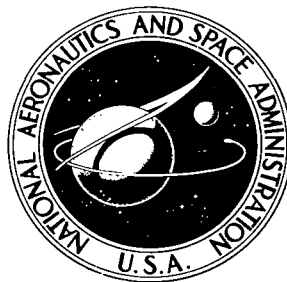


NASA TECHNICAL NOTE



NASA TN D-6383

c.1

NASA TN D-6383

LOAN COPY: RETURN  
AFWL (DOGL)  
KIRTLAND AFB, N.

0078490



TECH LIBRARY KAFB, NM

# CONSIDERATION OF SIMPLE MODEL ATOMS FOR ARGON DISCHARGE CALCULATIONS

*by James R. Rose and John V. Dugan, Jr.*

*Lewis Research Center*

*Cleveland, Ohio 44135*



0078490

1. Report No. <b>NASA TN D-6383</b>	2. Government Accession No.	3. Recipient's Catalog No.	
4. Title and Subtitle <b>CONSIDERATION OF SIMPLE MODEL ATOMS FOR ARGON DISCHARGE CALCULATIONS</b>		5. Report Date <b>June 1971</b>	
		6. Performing Organization Code	
7. Author(s) <b>James R. Rose and John V. Dugan, Jr.</b>		8. Performing Organization Report No. <b>E-6220</b>	
		10. Work Unit No. <b>129-02</b>	
9. Performing Organization Name and Address <b>Lewis Research Center National Aeronautics and Space Administration Cleveland, Ohio 44135</b>		11. Contract or Grant No.	
		13. Type of Report and Period Covered <b>Technical Note</b>	
12. Sponsoring Agency Name and Address <b>National Aeronautics and Space Administration Washington, D. C. 20546</b>		14. Sponsoring Agency Code	
		15. Supplementary Notes	
16. Abstract <p>Simple model atoms are useful for satisfactory calculation of plasma properties in gas discharges with low electron temperature <math>T_e</math>. Model atoms of 2-, 3-, and 5-levels give ionization fraction <math>f</math> in satisfactory agreement with 26-level results for cesium plasmas that are optically thick to resonance radiation. The calculation of nonequilibrium <math>f</math> values is extended to argon discharges of <math>T_e</math> values of 8000 and 11 605 K. The calculated values of <math>f</math> closely approximate the Saha predictions in the completely thick radiation limit. Level inversions are calculated at both <math>T_e</math> values for argon plasmas that are optically thick to resonance radiation.</p>			
17. Key Words (Suggested by Author(s)) <b>Model atom Argon discharges Rate equations Argon</b>		18. Distribution Statement <b>Unclassified - unlimited</b>	
19. Security Classif. (of this report) <b>Unclassified</b>	20. Security Classif. (of this page) <b>Unclassified</b>	21. No. of Pages <b>20</b>	22. Price* <b>\$3.00</b>

# CONSIDERATION OF SIMPLE MODEL ATOMS FOR ARGON DISCHARGE CALCULATIONS\*

by James R. Rose and John V. Dugan, Jr.

Lewis Research Center

## SUMMARY

Simple model atoms are useful for satisfactory calculation of plasma properties in gas discharges with low electron temperature  $T_e$ . Model atoms of 2-, 3-, and 5-levels give ionization fractions  $f$  in satisfactory agreement with 26-level results for cesium plasmas that are optically thick to resonance radiation. The calculation of nonequilibrium  $f$  values is extended to argon discharges of  $T_e$  values of 8000 and 11 605 K. The calculated values of  $f$  closely approximate the Saha predictions in the completely thick radiation limit. Level inversions are calculated at both  $T_e$  values for argon plasmas that are optically thick to resonance radiation.

## INTRODUCTION

Numerical values for free-electron distribution functions  $f_e(u)$  and electronic state populations  $N_L$  have been obtained for cesium-seeded argon discharges with low electron temperature  $T_e$  from simultaneous solution of the Boltzmann and rate equations (ref. 1). (Symbols are defined in the appendix.) The rate equations were solved for a 5-level cesium (Cs) model atom in reference 1, the ground electronic level plus four excited states. The limitations of 2-, 3-, and 5-level model atoms in predicting departures of electron number densities  $N_e$  from equilibrium (Saha) values were reported in reference 2. These results for an assumed Maxwellian  $f_e(u)$  were compared with results for a 26-level model (ref. 3). Where comparison is possible, the agreement is within a factor of 2 at low and high initial cesium number densities  $N_{Cs}$  but is only

---

\* Presented at the Second Arc Symposium sponsored by the American Physical Society, Hartford, Conn., October 20, 1970.

qualitative at intermediate and low cesium nuclei densities  $N_{\text{Cs}} (<10^{22} \text{ m}^{-3})$  for plasmas optically thick to resonance radiation.

The electron distribution functions calculated for cesium in reference 1 are near Maxwellian down to  $T_e = 2100 \text{ K}$  for plasmas optically thick to resonance radiation. Numerical difficulties were encountered for  $T_e < 2100 \text{ K}$ , where the iterative scheme for  $f_e(u)$  does not converge for the high-energy tail.

Simple model atoms serve two useful purposes: they allow for (1) convenient calculation of nonequilibrium  $N_e$  values in low  $T_e$  plasmas and (2) straightforward isolation of numerical difficulties that may occur in the solution for the troublesome high-energy tail of  $f_e(u)$  (refs. 1 and 2).

The purpose of this work is to investigate the usefulness of relatively simple (2-, 3-, and 5-level) argon model atoms in calculating  $N_e$  values for argon discharges. The electron distribution function is assumed to be Maxwellian. The ratio of the first excited state to ground state binding energy of argon is much different from that of cesium (0.26 and 0.64, respectively). This essential difference in the atomic structure of argon and the current interest in argon discharges warrants this separate investigation. The investigation entails calculating  $N_e$  values in argon discharges operating with electron temperatures of 8000 and 11 605 K (1 eV) for the 2-, 3-, and 5-level model atoms. The calculations were done for plasmas that are (1) thin to all radiation, (2) thick to resonance radiation, and (3) thick to all radiation. The thick to all radiation limit should approximate the Saha values of  $N_e$ .

## ATOMIC MODELS

The 2-, 3-, and 5-level model atoms are shown schematically in figure 1. The 5-level model consists of a ground state and four excited states. The lowest lying excited state is obtained by grouping all of the energy levels arising from the  $3p^5 4s$  electronic configuration (i.e., the  $4s^1 p_{1,0}$  and  $4s^3 p_{2,1}$  energy levels). Similarly, the second state is obtained by grouping the levels arising from the  $3p^5 4p$  electronic configuration and the third by grouping those states arising from the  $3p^5 5s$  and  $3p^5 3d$  configurations. Finally, all the remaining states are approximated by considering a continuum of states from the highest lying level of the  $3p^5 3d$  state to the ionization limit. The energy of the fifth level is taken to be the mean energy of this upper continuum of states. The degeneracy of the fifth level was chosen in the same manner as in the cesium studies (ref. 2). This level must approximate the presence of several thousand spectroscopic states in the absence of comparison with results for more detailed models. The Saha check calculations (completely thick to all radiation) and the nonequilibrium results of this report are quite insensitive to the degeneracy of the fifth level  $g_5$ . Values of

50, 200, and 500 were tried for  $g_5$ . The equation  $\dot{N}_e = 0$  was best satisfied for  $g_5 = 200$ , so the results are reported for this value. This is consistent with the manner in which the cesium results of reference 2 varied with the upper-level degeneracy.

The energy of the upper level of the 3-level atom is taken to be the mean energy of the highest lying level of the  $3p^5 4p$  electronic configuration and the ionization limit of argon. Its degeneracy is taken to be that of the  $3p^5 4p$  electronic configuration. The 2-level atom consists simply of the ground state and the  $3p^5 4s$  states of argon.

The binding energy of a given level is assigned as the mean energy of the multiplet it represents, that is,

$$E_L = \bar{E}_{Lj} = \frac{\sum_j g_{Lj} E_{Lj}}{\sum_j g_{Lj}} \quad (1a)$$

and the corresponding degeneracy is simply

$$g_L = \sum_j g_{Lj} \quad (1b)$$

Values of the  $E_{Lj}$  and  $g_{Lj}$  were obtained for argon from reference 4.

## ASSUMPTIONS AND ANALYSIS

The equations solved in the present work are the steady-state atomic rate equations and the mass conservation equation. The rate equation for the  $L$ th state, that is, the rate of change of the number of bound electrons in level  $L$ ,  $N_L$ , is (ref. 1)

$$\begin{aligned} \dot{N}_L = & -N_L(N_e \mathcal{H}_L + \mathcal{A}_L) + N_e \sum_{K \neq L} N_K K_{K \rightarrow L} \\ & + \sum_{K > L} N_K A_{K \rightarrow L} + N_e N_i \left[ (K_L^{\text{cap}})^* + \beta_L \right] \quad (\text{m}^{-3}) (\text{sec}^{-1}) \quad (2) \end{aligned}$$

In the steady state  $\dot{N}_L = 0$ .

In equation (2)  $K_{K \rightarrow L}$  ( $(m^3)(sec^{-1})$ ) is the rate coefficient for populating the Lth state by collisional excitation or deexcitation of the Kth state;

$\mathcal{H}_L \left( \equiv \sum_{K \neq L} K_{L \rightarrow K} + K_L^{ion} \right)$  ( $(m^3)(sec^{-1})$ ) is the rate coefficient for depopulating the Lth state by collisional excitation, deexcitation, and ionization;  $A_{K \rightarrow L}(sec^{-1})$  is the probability of a spontaneous radiative transition from the Kth state to the Lth state ( $K > L$ );

$\mathcal{A}_L \left( \equiv \sum_{K < L} A_{L \rightarrow K} \right)$  is the probability of spontaneous radiative transitions from the Lth state to lower states K;  $(K_L^{cap})^*$  ( $(m^3)(sec^{-1})$ ) is an effective two-body rate coefficient for capture into level L; and  $\beta_L$  ( $(m^3)(sec^{-1})$ ) is the rate coefficient for radiative capture into level L. Photoionization is ignored because of its unlikelihood. The mass conservation equation can be written approximately as

$$N_0 = N_i + \sum_L N_L \quad (m^{-3}) \quad (3)$$

where  $N_0$  is the initial argon number density. Equations (2) and (3) are solved for the electronic state populations  $N_L$  and the electron number density  $N_e (= N_i)$  for assigned values of both the argon initial number density  $N_0$  and the electron temperature  $T_e$ .

Boundary and spatial effects are neglected in the calculations and it is assumed that the electron distribution function is Maxwellian at the assigned temperature  $T_e$ . The later versions of the Gryzinski inelastic cross sections (ref. 5) are used to calculate the excitation and ionization rate coefficients. The corresponding inverse processes are then calculated by the principle of detailed balancing.

## Radiative Transition Probabilities

The resonance transition probability  $A_{2 \rightarrow 1}$  was obtained from reference 6. Approximate, scaled values of  $A_{2 \rightarrow 1}$  were used for the other resonance transitions, that is,

$$A_{K \rightarrow L} = \frac{g_2 (E_1 - E_K)^2}{g_K (E_1 - E_2)^2} A_{2 \rightarrow 1} \quad (sec^{-1}) \quad (4)$$

for  $K > 2$ . To obtain this expression it was assumed that the oscillator strengths for all resonance transitions are nearly the same and equal to the oscillator strength for the lowest resonance transition.

The value for  $A_{3-2}$  is the mean value of the thirty allowed transitions between the  $3p^5 4p$  and  $3p^5 4s$  multiplets (ref. 7). Other transition probabilities were either assigned approximately from comparison with similar transitions or calculated using the Coulomb approximation (ref. 8). A summary of the numerical values used for the  $A_{K-L}$  is given in table I.

## Radiative Capture Coefficients

The radiative capture coefficients  $\beta_L$  for the excited states ( $L > 1$ ) were calculated by detailed balancing using hydrogenic photoionization cross sections (ref. 9).

The ground state value of the radiative capture rate coefficient  $\beta_1$  was obtained from an experimental ground state photoionization cross section (ref. 10). This photoionization cross section was curve fitted against incident photon energy, and  $\beta_1$  was obtained from it by using the principle of detailed balancing.

The variation of the ionization fraction  $f$  in cesium plasmas has been discussed in terms of the source and sink terms in the electron conservation equation (ref. 3). The normalized expression for  $\dot{N}_e = 0$  is

$$f^2 \sum_{L=1}^M (K_L^{\text{cap}})^* + f \sum_{L=1}^M \beta_L = \sum_{L=1}^M K_L^{\text{ion}} n_L \quad (5)$$

where  $f \equiv N_e/N_0$  is the fraction ionized and  $n_L \equiv N_L/N_0$  is the normalized population of the  $L$ th electronic state. The quantity  $K_L^{\text{ion}}$  ( $(\text{m}^3) (\text{sec}^{-1})$ ) is the rate coefficient for ionization from the  $L$ th state. Although the equation for the ionization fraction, equation (5), appears to be simply quadratic in  $f$ , the normalized bound state populations  $n_L$  are strong functions of  $N_0$  and optical thickness for a given electron temperature.

The levels which are sources of ionization for the various model atoms can be determined from the net ionization rates. The net ionization rate from the  $L$ th electronic state can be written from equation (5) as

$$R_L^{\text{net}} = K_L^{\text{ion}} n_L - \left[ (K_L^{\text{cap}})^* f^2 + \beta_L f \right] \quad (\text{m}^3) (\text{sec}^{-1}) \quad (6)$$

The positive  $R_L^{\text{net}}$  values define states which are free electron sources and the negative  $R_L^{\text{net}}$  values define states which are free electron sinks. The behavior of the fraction

ionized as  $T_e$  and  $N_o$  are changed can generally be explained by observing the changes in  $R_L^{net}$ .

## RESULTS AND DISCUSSION

### Saha Check in Limit of Complete Optical Thickness

It is possible to perform a numerical check of the accuracy of a model atom in the limit of complete optical thickness. In this limit the true fraction ionized is that predicted by the Saha equation for argon, including all possible occupied electronic states. The results of this check showed that the 2-, 3-, and 5-level model atoms predict the Saha result to within 5 percent for all cases tried ( $T_e = 8000$  K, 11 605 K, and  $N_o = 10^{18}$  to  $10^{26}$ ).

### Optically Thin

The calculated fraction ionized for an optically thin plasma and a 1-eV electron temperature is plotted against initial argon number density in figure 2. The figure shows that the fraction ionized is generally much less than the Saha solution, although the 5-level model atom results approach the Saha results at the highest  $N_o$  values. The fraction ionized is constant for  $N_o$  values of  $10^{18}$  to  $10^{22} \text{ m}^{-3}$  for the 5-, 3-, and 2-level model atoms. The 5-level model atom predicts a sharp increase in the fraction ionized as  $N_o$  increases above  $10^{22} \text{ m}^{-3}$ . The 2- and 3-level model atom predictions of the fraction ionized remain relatively constant over the entire range of  $N_o$  values considered.

A better understanding of these fraction-ionized variations is obtained from examining figure 3. The figure shows the positive  $R_L^{net}$  values given by equation (6) scaled by a quantity  $R_{max}$ , which is the maximum sum obtained by adding the positive  $R_L^{net}$  values for each  $N_o$  value for the 5-level model atom calculations for given plasma radiation conditions. The quantity  $R_L^{net}/R_{max}$  is denoted by  $R'_L$ . This scaling by  $R_{max}$  correlates the behavior of the 5-level model atom results to the 2- and 3-level results. States that are free electron sinks are not shown in the figure. The apparent discontinuity in some of the curves is due to the lack of data between integral powers of  $N_o$ ; that is, a given curve starts at the lowest integral power of  $N_o$  for which it has a positive value.

As can be seen in figure 3, the value of  $R'_L$  is roughly constant and equal for all three model atoms in the  $N_o$  range of  $10^{18}$  to  $10^{22}$ , where the fraction ionized behaves

similarly (fig. 2). A look at the rates involved shows that in this range of  $N_0$  the fraction ionized predicted by the three model atoms considered corresponds to the coronal limit (ref. 11), that is,

$$f = \frac{\sum_{L=1}^M K_L^{\text{ion}} n_L}{\sum_{L=1}^M \beta_L} \quad (7)$$

It can be seen from equation (7) that generally in the coronal limit radiative capture balances collisional ionization. In the case of argon at these conditions only the ground state participates, so that

$$f \approx \frac{K_1^{\text{ion}} n_1}{\beta_1} \quad (8)$$

The reason for the sharp increase in  $f$  for the 5-level atom at higher  $N_0$  values is apparent from figure 3. All states except the ground state contribute increasingly to the free-electron population as  $N_0$  increases until maxima in the  $R_L'$  values ( $2 < L < 5$ ,  $M = 5$ ) are reached at the same value of  $N_0$  that  $f$  has a maximum. Also note the upper level is the main ionization source at the higher  $N_0$  values. For  $N_0 > 10^{24} \text{ m}^{-3}$  three-body capture becomes a more dominant process which causes all levels except the  $L = 5$  level to become electron sinks. It can be seen in figure 2 that there is a corresponding decrease in the fraction ionized.

It is clear that the upper level is populated by a ladder mechanism (ref. 2) in the 5-level case. Also, this fifth state has a relatively low binding energy (0.78 eV), so that once it is significantly populated it is readily ionized since  $kT_e > E_5$  for a 1-eV electron temperature. For 2- and 3-level model atoms there is no sharp increase in the fraction ionized as  $N_0$  increases, and the upper level never becomes a source of free electrons. The energy gap between the second and third levels of the 3-level atoms is so large that the collisional excitation rate of the third state from the second state is much less than the depopulation rate of the second state by spontaneous transitions to the ground state  $A_{2-1}$ . Thus, the ladder mechanism is inhibited for the simpler model atoms.

The results for  $T_e = 8000 \text{ K}$ , optically thin to all radiation (not shown) are roughly the same for the 5-, 3-, and 2-level atoms. The fraction ionized is roughly constant

over the entire range of  $N_0$  values considered ( $f = (5 \text{ to } 8) \times 10^{-8}$ ). The  $f$  curves remain flat because the excitation rate coefficients for populating even the lowest lying excited states are small compared to the corresponding values at  $kT_e = 1 \text{ eV}$ . Thus, the states which are relatively easily ionized once populated never become significantly populated.

## Optically Thick to Resonance Radiation

Population inversion. - For plasmas optically thick to resonance radiation the phenomenon of population inversion ( $n_4 > n_3$ ) occurs for both electron temperatures considered (8000 and 11 605 K). The normalized excited state number densities  $n_L$  for the 5-level atom are displayed against  $N_0$  in figure 4 for  $kT_e = 1 \text{ eV}$  (11 605 K) and in figure 5 for  $T_e = 8000 \text{ K}$ . The figures also show the curve of  $n_2$  against  $N_0$  calculated for thick to all radiation conditions  $n_{2, \text{Saha}}$ . As can be seen in figures 4 and 5, the level inversion ( $n_4 > n_3$ ) occurs in the range where  $n_2$  is greater than or not much less than  $n_{2, \text{Saha}}$ . When the population of the  $L = 2$  level is this large, it can readily populate states above it by excitation. Excitation from the  $L = 2$  state is the largest contributor to the populations of both the  $L = 3$  and  $L = 4$  states. The third level ( $L = 3$ ), however, is more readily depopulated than the  $L = 4$  level by spontaneous radiative transitions. The other depopulating mechanisms for these states are relatively small at the lower  $N_0$  values. Thus, as the  $L = 4$  and  $L = 3$  states become populated, the  $L = 3$  state is preferentially depopulated by spontaneous transitions, and this depopulation in turn leads to  $n_4 > n_3$  over a range of  $N_0$  values.

As  $N_0$  increases, however, the electron density  $N_e (= fN_0)$  increases, depopulation by spontaneous transitions is overshadowed by collisional depopulating mechanisms, and the population inversion no longer occurs. Since the collisional depopulating mechanisms depend on  $N_e$ , one might expect the population inversion to occur up through higher  $N_0$  values for  $T_e = 8000 \text{ K}$  (where the fraction ionized is relatively small) than for  $kT_e = 1 \text{ eV}$  (11 605 K). Figures 4 and 5 show this to be the case.

Figure 4 shows  $n_5 > n_4$  for  $N_0$  values greater than  $10^{23} \text{ m}^{-3}$ . This evident level inversion is probably due to the artificial manner in which the  $L = 5$  level is constructed, and there is no physical interpretation given for this.

Fraction-ionized variation. - Energy equivalent of electron temperature, 1 eV (11 605 K): The fraction ionized is plotted against initial argon number density for plasmas thick to resonance radiation in figure 6 for  $kT_e = 1 \text{ eV}$  (11 605 K). The  $f$  values predicted by the 2- and 5-level atoms are roughly the same at low and high  $N_0$  values. At intermediate  $N_0$  values the 5-level atom predicts  $f$  values up to 50 percent higher than either the 2- or 3-level atom. At the higher  $N_0$  values ( $> 10^{24} \text{ m}^{-3}$ ) three-

body capture becomes the dominant capture process which causes the fraction ionized to decrease. This decrease in  $f$  is much more pronounced for the 3-level atom than for either the 2- or 5-level atom. All model atoms predict fractions ionized much below the Saha values except at the highest  $N_0$  values where the dominant atomic processes are collisional and Saha equilibrium is approached.

The  $f$  curves for the 2- and 3-level atoms can be predicted by equation (7) (thick coronal limit) in the range  $N_0 = 10^{18} - 10^{22} \text{ m}^{-3}$ . In particular, though,

$$f \approx \frac{n_2 K_2^{\text{ion}}}{\beta_1}$$

in this range of  $N_0$ .

Figure 7 shows the normalized ionization rates against the initial argon number density for the various model atoms for a 1-eV electron temperature and plasmas thick to resonance radiation. These correspond to the fraction-ionized curves shown in figure 6. In the case of the 5-level atom all states except the ground state are contributors to the free-electron population over most of the range of  $N_0$  values, and the normalized ionization rates roughly follow the trends of the fraction-ionized curve (fig. 6). Similar remarks apply to the normalized ionization rate curve for the 2-level model atoms.

It is seen from figure 7 that the ionization rate curve for the 3-level atom increases as  $N_0$  increases for  $N_0 > 10^{23} \text{ m}^{-3}$ . This obviously does not explain the rapid decrease in the fraction ionized for the 3-level atom in the same region (fig. 6). The reason for this rapid decrease in  $f$  is that in this region the dominant atomic rate is the three-body capture rate into the upper level of the atom.

Electron temperature, 8000 K: The fraction ionized is plotted against initial argon number density in figure 8 for  $T_e = 8000 \text{ K}$  and the plasmas optically thick to resonance radiation. Qualitatively the results are similar to the corresponding results for  $kT_e = 1 \text{ eV}$  (11 605 K) except that the curves are shifted to higher  $N_0$  values.

The normalized ionization rates plotted against initial argon number density for the 8000 K electron temperature (fig. 9) show the same shift relative to the corresponding  $kT_e = 1 \text{ eV}$  (11 605 K) results (see fig. 7).

## Effect of Optical Transparency

Figures 10 and 11 show the effect of the optical transparency of the plasma on the fraction ionized. The curves are the ratios of the calculated values of the fraction ionized for the 5-level atom to the fraction ionized predicted by the Saha equation for

electron temperatures of 8000 and 11 605 K, respectively. The curves for plasmas thick to all radiation are very nearly horizontal and show the accuracy of the 5-level model atom in this completely thick limit. Comparison of figures 10 and 11 shows that for a given plasma optical thickness the plasma is farther from equilibrium at the lower temperature. The figures also indicate a trend toward equilibrium as  $N_0$  increases, as should be the case.

## CONCLUDING REMARKS

Calculations made using 2-, 3-, and 5- level argon model atoms indicate that these simple model atoms are useful in predicting the fraction ionized in argon discharges. All three model atoms predict the expected coronal limit at low initial argon number densities  $N_0$ . At high  $N_0$  the results for the 5-level atom approach the Saha limit, which is the limiting solution for this condition. The accuracy of these simple model atoms at intermediate  $N_0$  values is difficult to assess because of the lack of other data for comparison.

The 5-level argon model atom proved useful in interpreting level inversions that occurred at both temperatures used in the calculations (8000 and 11 605 K) for plasmas thick to resonance radiation.

Simple model atoms are also useful for isolating numerical difficulties that may occur in the numerical solution of the Boltzmann equation in regions where inelastic collision effects are not negligible.

Lewis Research Center,  
National Aeronautics and Space Administration,  
Cleveland, Ohio, March 29, 1971,  
129-02.

## APPENDIX - SYMBOLS

$A_{L \rightarrow K}$	probability of spontaneous radiative transition $L \rightarrow K$ , $\text{sec}^{-1}$
$\mathcal{A}_L$	$\sum_{K < L} A_{L \rightarrow K}$
$E_L$	binding energy of level $L$ , eV
$f$	fraction ionized
$f_e(u)$	electron energy distribution function
$g_L$	degeneracy of level $L$
$K_{L \rightarrow K}$	rate coefficient for collision-induced transition $L \rightarrow K$ , $(\text{m}^3) (\text{sec}^{-1})$
$(K_L^{\text{cap}})^*$	effective two-body rate coefficient for capture into level $L$ , $(\text{m}^3) (\text{sec}^{-1})$
$K_L^{\text{ion}}$	rate coefficient for ionization from level $L$ , $(\text{m}^3) (\text{sec}^{-1})$
$\mathcal{K}_L$	$\sum_{K \neq L} K_{L \rightarrow K} + K_L^{\text{ion}}$
$kT_e$	energy equivalent of electron temperature, eV
$N$	number density
$n_L$	dimensionless number density of $L$ th level
$R_L^{\text{max}}$	maximum ionization rate from level $L$ for 5-level model atom, $(\text{m}^3) (\text{sec}^{-1})$
$R_L^{\text{net}}$	net ionization (capture) rate of level $L$ , $(\text{m}^3) (\text{sec}^{-1})$
$R'_L$	scaled net ionization rate, $R_L^{\text{net}}/R_L^{\text{max}}$
$T_e$	electron temperature, K
$\beta_L$	rate coefficient for radiative capture into level $L$ , $(\text{m}^3) (\text{sec}^{-1})$
Subscripts:	
Cs	cesium
e	electron
i	ion
K, L	atomic level indices
M	upper level
max	maximum



o initial number density

Superscripts:

cap capture

ion ionization

time derivative

## REFERENCES

1. Dugan, J. V., Jr.; Lyman, F. A.; and Albers, L. U.: Solution of the Boltzmann and Rate Equations for the Electron Distribution Function and State Populations In Nonequilibrium MHD Plasmas. *Electricity from MHD. Vol. II. International Atomic Energy Agency, 1966, pp. 85-100. (Discussion, pp. 10-15.)*
2. Dugan, John V., Jr.: The Selection of Simple Model Atoms for Calculations of Electron Density In Nonequilibrium, Low Temperature Cs Plasmas. Presented at the 27th Annual Conference for Physical Electronics, Massachusetts Inst. Tech., Cambridge, Mass., Mar. 20-22, 1967.
3. Norcross, D. W.; and Stone, P. M.: Recombination, Radiative Energy Loss and Level Populations in Nonequilibrium Cesium Discharges. *J. Quantitat. Spectrosc. Radiat. Transfer*, vol. 8, no. 1, Feb. 1968, pp. 655-684.
4. Moore, Charlotte E.: Atomic Energy Levels. *Circ. 467, Vol. I, National Bureau of Standards, June 15, 1949.*
5. Gryziński, Michal: Classical Theory of Atomic Collisions. I. Theory of Inelastic Collisions. *Phys. Rev.*, vol. 138, no. 2A, Apr. 19, 1965, pp. 336-358.
6. Gruzdev, P. F.: Oscillator Strengths of Resonance Lines In the Spectra of NeI, ArI, KrI, XeI, Atoms and Na II and Rb II Ions. *Optics and Spectroscopy*, vol. 22, no. 2, Feb. 1967, pp. 170-171.
7. Garstang, R. H.; and Van Blerkom, Janet: Transition Probabilities in the Ar I Spectrum. *Opt. Soc. Am.*, vol. 55, no. 9, Sept. 1965, pp. 1054-1057.
8. Bates, D. R.; and Damgaard, Agnete: The Calculation of the Absolute Strengths of Spectral Lines. *Phil. Trans. Roy. Soc. (London), Ser. A*, vol. 242, no. 842, 1949, pp. 101-122.
9. Bates, D. R.: Atomic and Molecular Processes. Academic Press, 1962.
10. McDaniel, Earl W.: Collision Phenomena in Ionized Gases. John Wiley & Sons, Inc., 1964, p. 247.
11. Huddleston, Richard H.; and Leonard, Stanley L., eds.: Plasma Diagnostic Techniques. Academic Press, 1965, p. 208.

TABLE I. - TRANSITION PROBABILITIES AND BINDING ENERGIES FOR 5-LEVEL ATOM

Energy level, L	Energy level, K				Binding energy, $E_L$ , eV
	2	3	4	5	
	Radiation transition probability, $A_{K-L}$ , $\text{sec}^{-1}$				
1	$11.0 \times 10^7$	$4.55 \times 10^7$	$2.69 \times 10^7$	$1.09 \times 10^7$	15.75
2	-----	1.22	.05	1.00	4.11
3	-----	-----	.017	.50	2.58
4	-----	-----	-----	-----	1.65
5	-----	-----	-----	-----	.78

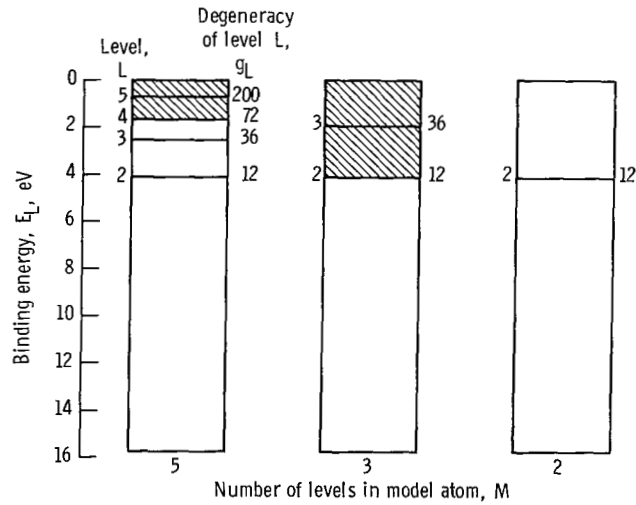


Figure 1. - Schematic diagram of argon model atoms.

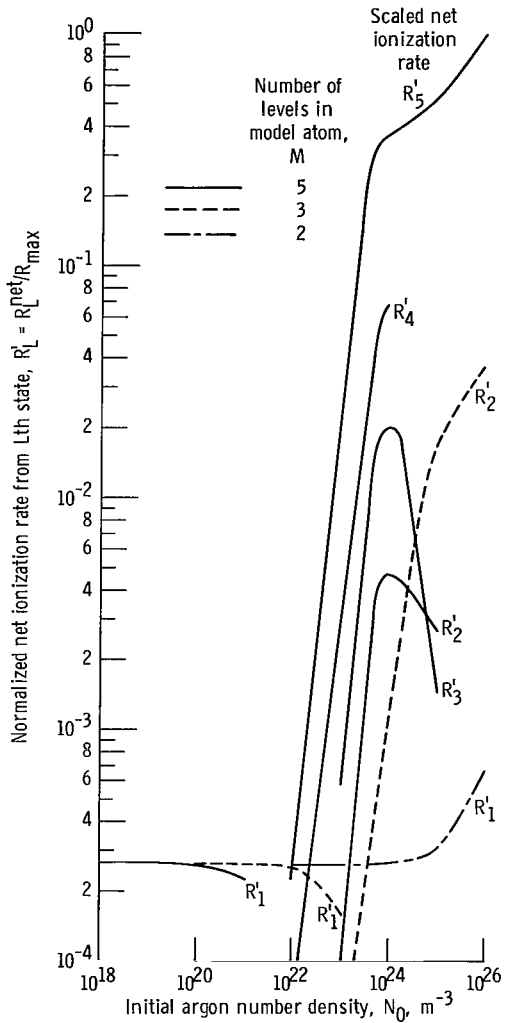


Figure 3. - Normalized net ionization rate from Lth state as function of initial argon number density. Energy equivalent of electron temperature, 1 eV (11 605 K); plasma thin to all radiation.

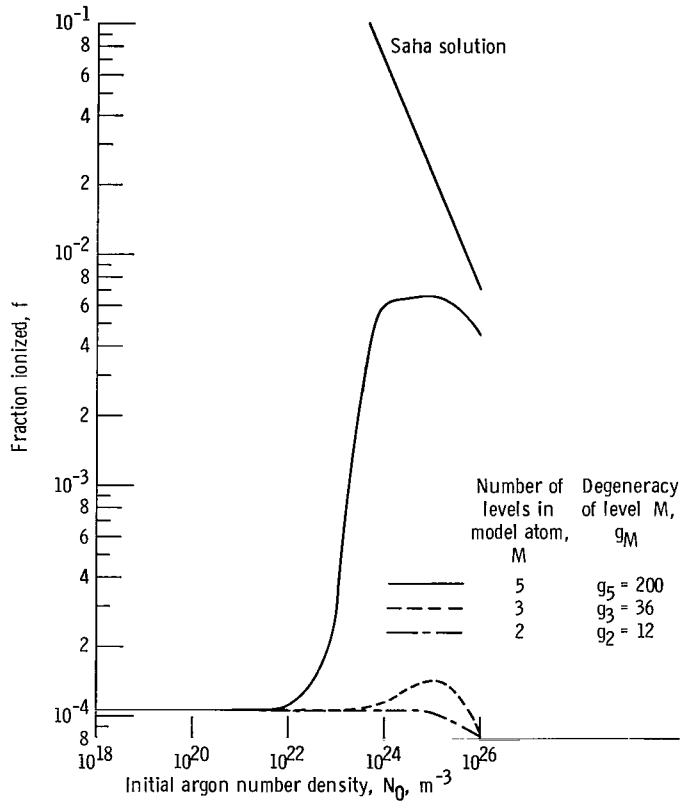


Figure 2. - Fraction ionized as function of initial argon number density. Energy equivalent of electron temperature, 1 eV (11 605 K); plasma thin to all radiation.

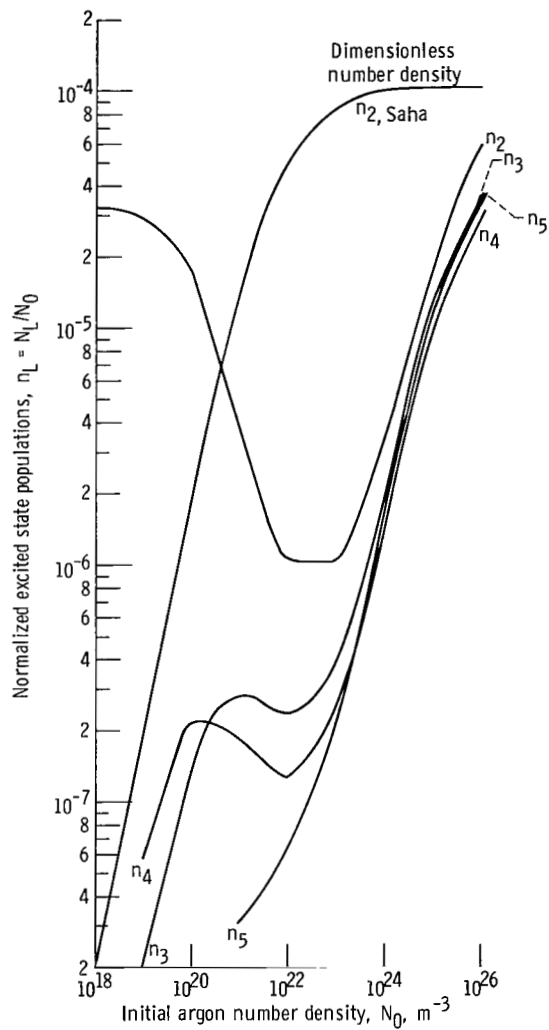


Figure 4. - Normalized excited state population as function of initial argon number density for 5-level model atom. Energy equivalent of electron temperature, 1 eV (11 605 K); plasma thick to resonance radiation.

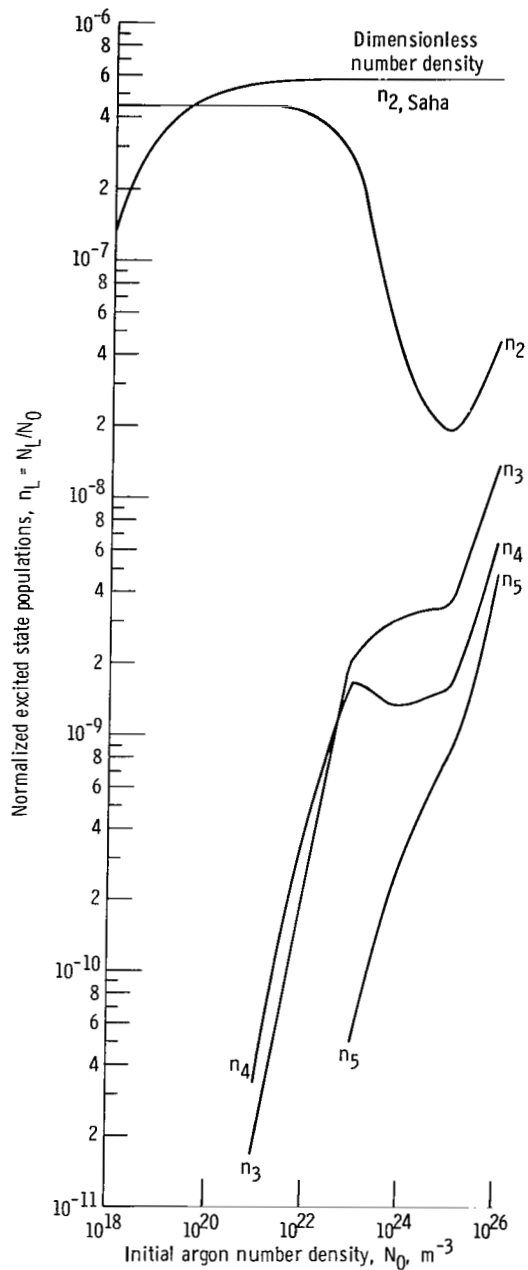


Figure 5. - Normalized excited state populations as function of initial argon number density for 5-level model atom. Electron temperature, 8000 K; plasma thick to resonance radiation.

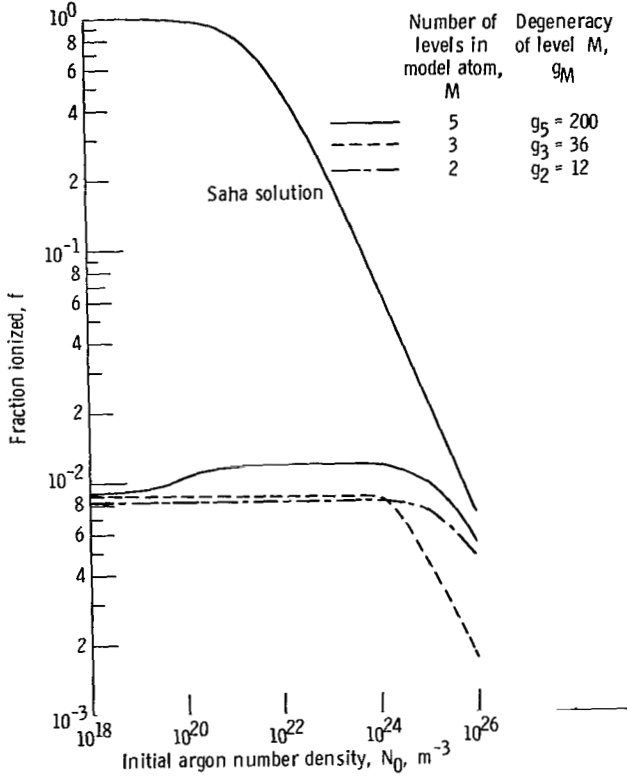


Figure 6. - Fraction ionized as function of initial argon number density. Energy equivalent of electron temperature, 1 eV (11 605 K); plasma thick to resonance radiation.

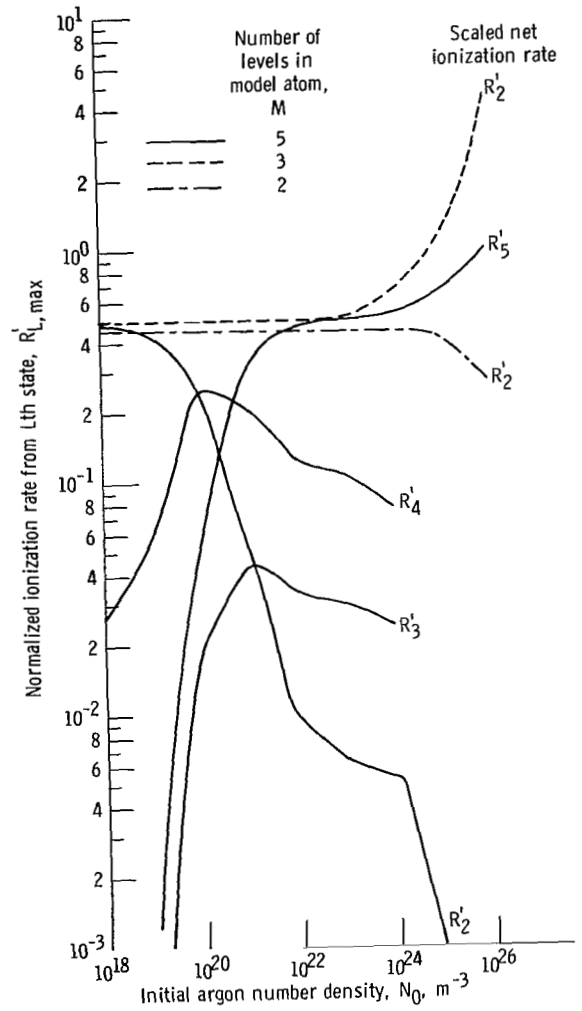


Figure 7. - Normalized net ionization rate from  $L$ th state as function of initial argon number density. Energy equivalent of electron temperature, 1 eV (11 605 K); plasma thick to resonance radiation.

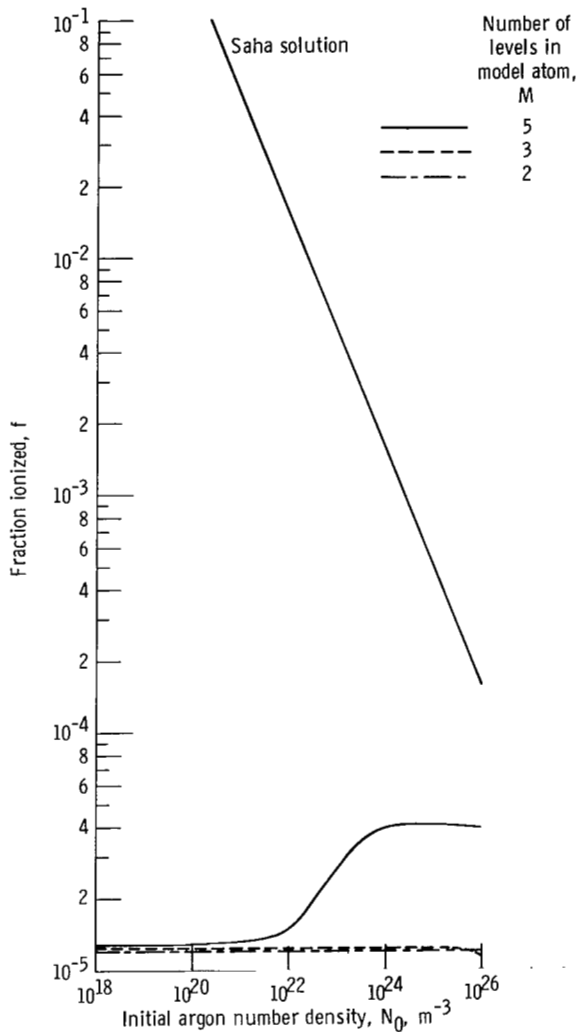


Figure 8. - Fraction ionized as function of initial argon number density. Electron temperature, 8000 K; plasma thick to resonance radiation.

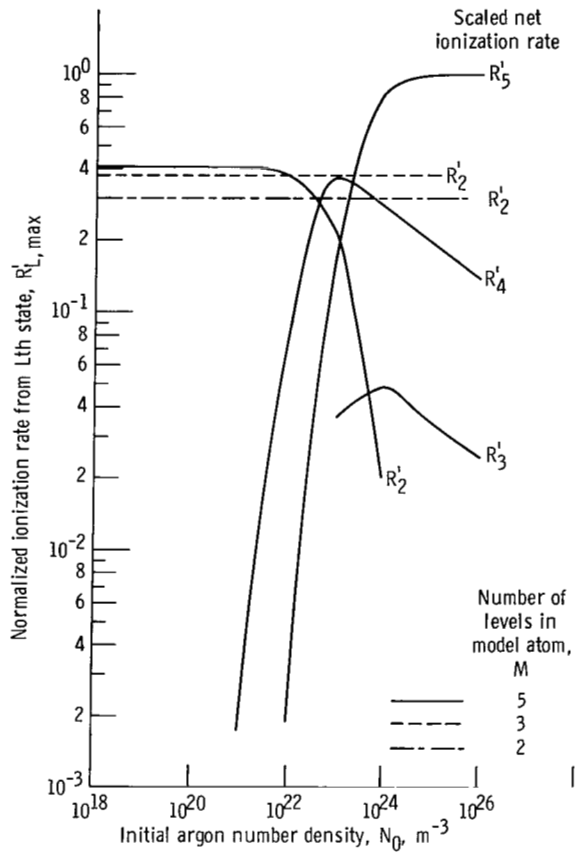


Figure 9. - Normalized net ionization rate from  $L$ th state as function of initial argon number density. Electron temperature, 8000 K; plasma thick to resonance radiation.

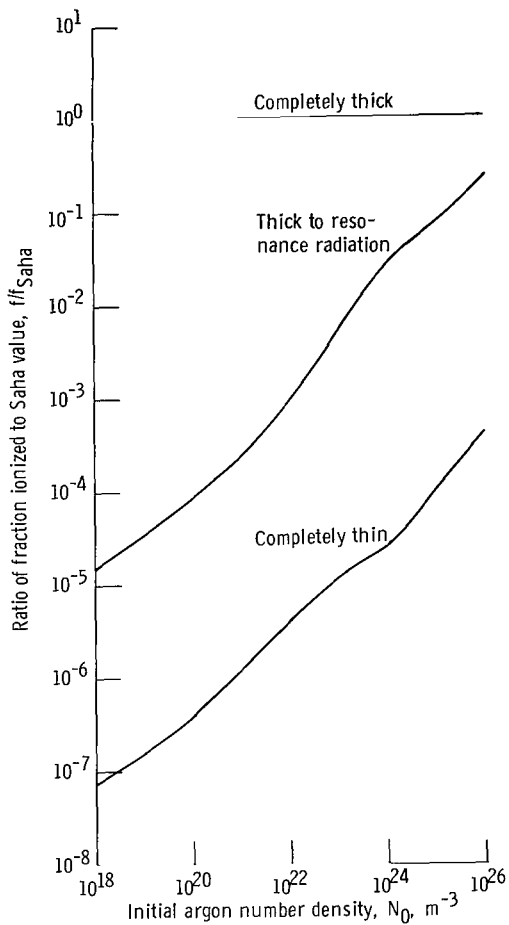


Figure 10. - Ratio of calculated fraction ionized to Saha fraction ionized for various plasma optical conditions. Electron temperature, 8000 K.

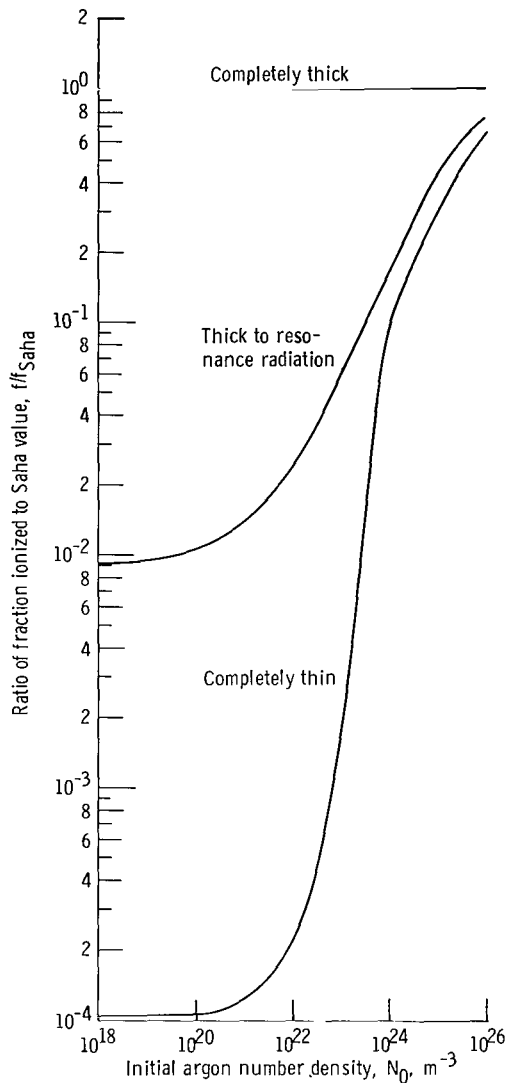


Figure 11. - Ratio of calculated fraction ionized to Saha fraction ionized for various plasma optical conditions. Energy equivalent of electron temperature, 1 eV (11 605 K).

NATIONAL AERONAUTICS AND SPACE ADMINISTRATION

WASHINGTON, D. C. 20546

OFFICIAL BUSINESS

PENALTY FOR PRIVATE USE \$300

FIRST CLASS MAIL



POSTAGE AND FEES PAID  
NATIONAL AERONAUTICS AND  
SPACE ADMINISTRATION

08U 001 49 51 3DS 71166 00903  
AIR FORCE WEAPONS LABORATORY /WLOL/  
KIRTLAND AFB, NEW MEXICO 87117

ATT E. LOU BOWMAN, CHIEF, TECH. LIBRARY

POSTMASTER: If Undeliverable (Section 158  
Postal Manual) Do Not Return

*"The aeronautical and space activities of the United States shall be conducted so as to contribute . . . to the expansion of human knowledge of phenomena in the atmosphere and space. The Administration shall provide for the widest practicable and appropriate dissemination of information concerning its activities and the results thereof."*

— NATIONAL AERONAUTICS AND SPACE ACT OF 1958

## NASA SCIENTIFIC AND TECHNICAL PUBLICATIONS

**TECHNICAL REPORTS:** Scientific and technical information considered important, complete, and a lasting contribution to existing knowledge.

**TECHNICAL NOTES:** Information less broad in scope but nevertheless of importance as a contribution to existing knowledge.

**TECHNICAL MEMORANDUMS:** Information receiving limited distribution because of preliminary data, security classification, or other reasons.

**CONTRACTOR REPORTS:** Scientific and technical information generated under a NASA contract or grant and considered an important contribution to existing knowledge.

**TECHNICAL TRANSLATIONS:** Information published in a foreign language considered to merit NASA distribution in English.

**SPECIAL PUBLICATIONS:** Information derived from or of value to NASA activities. Publications include conference proceedings, monographs, data compilations, handbooks, sourcebooks, and special bibliographies.

**TECHNOLOGY UTILIZATION PUBLICATIONS:** Information on technology used by NASA that may be of particular interest in commercial and other non-aerospace applications. Publications include Tech Briefs, Technology Utilization Reports and Technology Surveys.

*Details on the availability of these publications may be obtained from:*

**SCIENTIFIC AND TECHNICAL INFORMATION OFFICE**

**NATIONAL AERONAUTICS AND SPACE ADMINISTRATION**

Washington, D.C. 20546